Journal of Nuclear Materials 633 (2026) 156998

Contents lists available at ScienceDirect

Journal of Nuclear Materials

journal homepage: www.elsevier.com/locate/jnucmat

Tensile and Charpy impact properties of EUROFER97-3 and three RAFM steels after neutron irradiation at 330 ºC and 540 ºC to damage doses of 19-24 dpa

Vladimir Chakin [a,*], Carsten Bonnekoh [a], Ramil Gaisin [a], Rainer Ziegler [a], Michael Duerrschnabel [a], Michael Klimenkov [a], Hans-Christian Schneider [a], Rolf Rolli [a], Bronislava Gorr [a], Michael Rieth [a], Dmitry Terentyev [b], Jean Henry [c], Takashi Nozawa [d]

[a] Karlsruhe Institute of Technology (KIT), Institute for Applied Materials, 76131, Karlsruhe, Germany
[b] Belgian Nuclear Research Centre, SCK CEN, Mol, 2400, Belgium
[c] CEA, DEN, Service de Recherches Metallurgiques Appliquées, Laboratoire d'Analyse, Microstructurale des Matériaux, Université Paris-Saclay, 91191, Gif-sur-Yvette, France
[d] National Institutes for Quantum Science and Technology, Rokkasho, Aomori, Japan

A R T I C L E I N F O

Keywords:
RAFM steels
Radiation hardening
Radiation embrittlement
Upper shelf energy
Ductile-brittle transition temperature
Neutron irradiation

A B S T R A C T

The reduced-activation ferritic–martensitic (RAFM) steels EUROFER97-3 subjected to two heat treatments (EUROFER97-3_980/780 and EUROFER97-3_1100/700), F82H, as well the experimental heats M474, and L664B were irradiated in the BOR-60 fast reactor at temperatures of 330 °C and 540 °C, with damage doses ranging from 19.2 to 23.8 dpa. The results for all steels revealed a significant impact of irradiation temperature on tensile properties. Irradiation at 330 °C led to strong hardening and a pronounced reduction in uniform elongation, whereas irradiation at 540 °C resulted in practically no changes in tensile properties. In addition, a significant decrease in the upper shelf energy (USE) and a large shift in the ductile–brittle transition temperature (DBTT) was observed after irradiation of EUROFER97-3 with both heat treatments at 330 °C, while no significant changes in Charpy impact properties after irradiation at 540 °C were detected. In essence, irradiation at 540 °C caused only minor changes in the USE and DBTT of all studied RAFM steels compared with the unirradiated condition.

1. Introduction

EUROFER97-3 is the third industrial batch (or generation) of EUROFER97 steel and is the result of extensive R&D efforts at KIT (formerly FZK), which aimed at developing a reduced-activation ferritic–martensitic (RAFM) steel for use as structural materials for the European DEMO breeding blanket [1–5]. The development of the EUROFER-type RAFM steels can be roughly divided into three generations, each corresponding to a period of research progress and specific improvements in composition and microstructure. Generation 1 as early RAFM steels (≈ late 1970s – late 1980s) emerged when fusion programs began investigating low-activation structural materials. The major measures included modification of conventional 9–12 % Cr ferritic–martensitic steels leading to the replacement of high-activation alloying elements such as Mo to W and Nb to Ta as well as strong reduction of impurity elements such as Ni, Mo, Cu, and N. This resulted in the development of the first reduced-activation steel composition (e. g., MANET in Europe). Generation 2 of EUROFER97 reference steel (≈ early 1990s – early 2000s) consolidated earlier RAFM research and developed a standard reference material within European fusion programs. Major measures included development and standardization of EUROFER97 (around 1995–1997), optimized composition (~9 % Cr with W, V, Ta additions), improved thermo-mechanical processing and heat treatment such as austenitization (~980 °C) and tempering (~760 °C) with formation of a tempered martensitic lath microstructure, improved control of grain size and impurities. One of the main goals was to reduce the amount of long-term radioactive waste after neutron irradiation. EUROFER97-2 became the European reference structural

* Corresponding author.
E-mail address: vladimir.chakin@kit.edu (V. Chakin).

https://doi.org/10.1016/j.jnucmat.2026.156998
Received 31 December 2025; Received in revised form 24 May 2026; Accepted 15 August 2026
Available online 16 August 2026

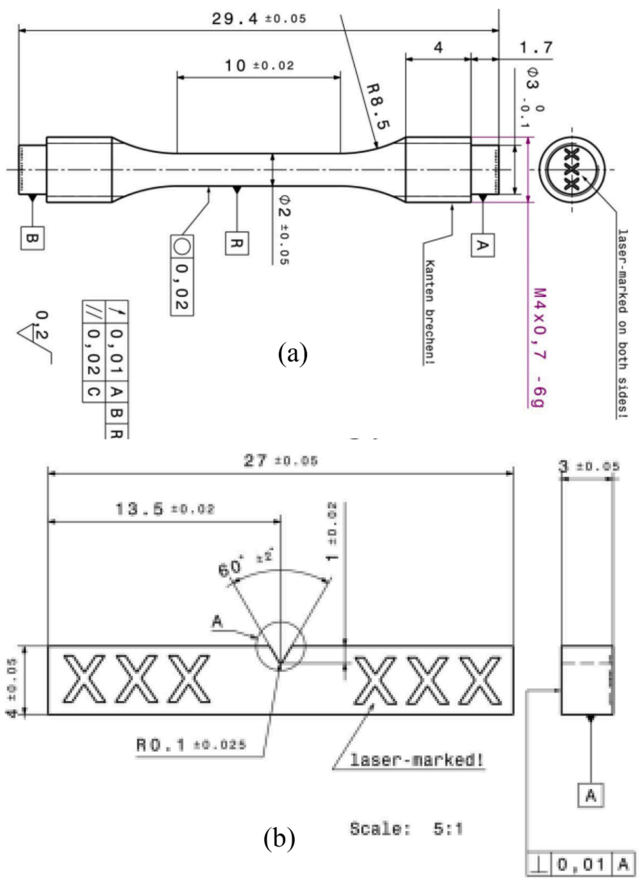

Fig. 1. Tensile (a) and impact bending (Mini-Charpy) (b) specimen for irradiation testing in the BOR-60 reactor.

Table 1
Heat treatments of the EUROFER97-3 grades.

Grade	Austenitization	Quenching	Tempering	Final cooling
EUROFER97-3_1100/700	1100 °C, 0.5 h	air	700 °C, 2 h	air
EUROFEF97-3_980/780	980 °C, 0.5 h	air	780 °C, 2 h	air

Table 2
Chemical composition of EUROFER97-3 in wt.%.

Element	Specification	Analysis
Cr	8.50-9.50	9.00±0.19
C	0.090-0.120	0.102±0.009
N	0.015-0.045	0.0350±0.0074
O	0.01	0.0004±0.0001
B	0.002	0.0004±0.0001
Al	0.01	0.0015±0.0003
Si	<0.05	0.0184±0.0008
P	0.005	0.0017±0.0003
Ti	<0.02	0.00018±0.00002
V	0.15-0.25	0.2117±0.0044
Mn	0.20-0.60	0.529±0.009
Fe	Not defined	87.5 ± 2.6
Co	0.01	0.0020±0.0003
Ni	0.01	0.0099±0.0005
Cu	0.01	0.0015±0.0002
Nb	0.005	<0.0004
Mo	0.005	0.0021±0.0003
Ta	0.10-0.14	0.125
W	1.0-1.2	1.152±0.040

material for fusion blanket components (ITER test blanket modules, DEMO blanket). Generation 3 as advanced EUROFER97 variants was created by ≈ mid-2000s to present. The research shifted toward improving high-temperature capability and radiation tolerance for DEMO fusion reactors and included measures such as oxide dispersion strengthened (ODS) EUROFER97 with nano-oxide particles (e.g., Y_2O_3), advanced thermo-mechanical treatments for ultra-fine grain structures, improved creep resistance and irradiation stability. A main goal is an increase operating temperature from ~550 °C to ~600–650 °C improving radiation damage tolerance for long-term fusion operation.

The EUROFER97-3 batch in this study was produced within the framework of the Test Blanket Module (TBM) program [6].

In addition to EUROFER97-3, three other RAFM steels were investigated such as F82H, M474, and L664B, which were developed by QST (Japan), SCK CEN (Belgium), and CEA (France), respectively.

Within the broader DEMO materials development roadmap, EUROFER97-3 was scheduled to undergo a comprehensive evaluation of key mechanical properties, including tensile strength and ductility, Charpy impact behavior, creep, low-cycle fatigue, and fracture toughness after neutron irradiation. These irradiation experiments were conducted in the BOR-60 fast reactor, which provides high fast-neutron fluxes, enabling damage doses of approximately 20 dpa for the initial DEMO blanket set and 40–50 dpa for the subsequent set within irradiation campaigns of roughly two and four years, respectively [7]. At present, RAFM steel specimens have already been irradiated up to 20 dpa, while irradiation to 40 dpa is ongoing.

Irradiation temperatures of 325 °C and 550 °C were selected to represent the lower and upper operational temperature bounds of both the HCPB (Helium-Cooled Pebble Bed) and WCLL (Water-Cooled Lithium-Lead) DEMO breeding blanket concepts.

The objective of this study is to assess the effects of neutron irradiation to a dose of 20 ± 2 dpa at target temperatures of 325 ± 10 °C and 550 ± 20 °C on the tensile and Charpy impact properties of the RAFM steels EUROFER97-3, F82H, M474, and L664B.

2. Experimental

2.1. Materials, specimens, heat treatment

2.1.1. EUROFER97-3

The EUROFER97-3 plate (ID45) used in this work (dimensions: 1015 × 532 × 33.3 mm) was produced by Saarschmiede Freiformschmiede GmbH through a manufacturing route consisting of:

- primary melting in a vacuum induction furnace;
- secondary melting via vacuum arc remelting;
- forging to a billet of roughly Ø150 × 700 mm;
- cropping of the billet's top and bottom ends to remove surface and forging defects;
- subsequent rolling on a trio mill to plate form;
- quality heat treatment.

Tensile [8] (Fig. 1a) and Mini-Charpy (KLST) impact bending [9] (Fig. 1b) specimens were machined from this plate together with creep [10] specimens. Two sets of the tensile and Charpy impact specimens were produced, each subjected to a different heat-treatment schedule (see Table 1) at KIT. All specimens were oriented such that the rolling direction lay perpendicular to the specimen axis.

The chemical composition of EUROFER97-3 is presented in Table 2. Measurements performed at KIT (see the third column) show that the material meets the specified delivery requirements (second column in Table 2).

2.1.2. F82H

This steel was normalized at 960 °C for 30 min, followed by tempering at 750 °C for 60 min, with final air cooling. Table 3

Table 3
Chemical composition of F82H in wt.%.

Element	Analysis
Cr	8.00
C	0.091
N	0.016
O	0.001
B	0.002
Al	<0.007
Si	0.17
P	0.009
Ti	<0.003
V	0.19
Mn	0.46
Fe	balance
Co	<0.01
Ni	<0.01
Cu	0.0015±0.0002
Nb	<0.005
Mo	<0.01
Ta	0.03
W	1.88

Table 4
Hot rolling schedule for M474.

Hot rolling	Reduction, %	Temperature, C	Final thickness, mm
Initial	-	1200	70
Pass 1	19.5	1200	56
Pass 2	25	1150	42
Pass 3	30	1100	30
Pass 4	30	960	21
Pass 5	30	900	14
Pass 6	30	850	10

Table 5
Chemical composition of M474 in wt.%.

Element	Analysis
Cr	9.124
C	0.112
N	0.00123
O	0.0014
Al	0.0063
Si	0.006
P	0.0062
Ti	0.0014
V	0.24
Mn	0.408
Fe	89.004
Ni	0.005
Cu	0.0063
Nb	0.002
Mo	0.0018
Ta	0.085
W	0.977

Table 6
Hot rolling schedule for L664B.

Hot rolling	Reduction, %	Temperature, °C	Final thickness, mm
Initial	-		90
Pass 1	15	1100	77
Pass 2	15	1080	65
Pass 3	20	1050	52
Pass 4	20	1000	42
Pass 5	20	950	33
Pass 6	18	900	27
Pass 7	18	850	22
Air cooling to RT			

Table 7
Chemical composition of L664B in wt.%.

Element	Specification	Analysis
Cr	8.50-9.50	8.888
C	0.090-0.120	0.1053
N	0.005-0.015	0.0082
B	0.0105-0.0175	0.0144
V	0.17-0.23	0.222
Mn	0.90-1.10	0.9850
Ta	0.10-0.14	0.097
W	0.10-0.14	0.097
Si	< 0.05	0.0321
P	<0.005	0.0037
S	<0.005	0.0016
Al	<0.015	0.0034
Ti	<0.02	0.005
Nb	<0.0075	0.001
Cu	<0.02	0.0107
Ni	<0.025	0.006
O	<0.01	0.0086
Mo	<0.0075	0.0026
Co	<0.0015	0.0015

summarizes the chemical composition of F82H.

2.1.3. M474

The M474 casting initially weighed approximately 100 kg. After removal of the ingot head, which contained porosity, approximately 55–60 kg of material remained. A slice a few millimeters thick was cut from the ingot, and the chemical composition was determined from the center of this slice.

The casting was then sectioned into pieces with approximate dimensions of 120 × 120 × 70 mm^3. These blocks were heated to 1200 °C for 1 h and hot-rolled according to the rolling schedule shown in Table 4.

M474 is called “Lab–cast EUROFER (M474)” in [11]. The heat treatment of the “Lab–cast EUROFER (M474)” was 880 °C for 30 min + WQ (water quenching) 750 °C for 120 min + AC (air cooling).

The chemical composition of M474 is shown in Table 5.

2.1.4. L664B

Seven melts were produced in a vacuum induction furnace as 100 kg ingots. After removal of the hot top, which contained casting cavities, approximately 60 kg of usable material remained. The hot-rolling schedule for L664B is presented in Table 6.

The chemical composition was determined by WD-XRF and combustion analysis (for C, S, N, and O). Trace impurities were additionally verified by ICP analysis, performed since WD-XRF is not sufficiently accurate at such low concentrations. The analyzed compositions are given in Table 7.

L664B was normalized at 1000 °C for 30 min. Subsequently, all sheets were tempered at 760 °C for 90 min and then removed from the furnace to cool in air.

2.2. Electron backscatter diffraction (EBSD) and Vickers mictohardness characterization

The EBSD method was employed to obtain the inverse pole figure (IPF-Z) orientation maps projected along the surface normal. The analysis was performed using OIM 8 software. Grain boundaries are indicated by black lines. The grain size was defined as the equivalent circle diameter of areas enclosed by high-angle grain boundaries (HAGBs, misorientation angle > 15°), which approximates the martensitic lath packet size. Reconstruction of prior austenite grains (PAGs) was performed using the Nishiyama-Wasserman orientation relationship with a tolerance angle of 5°

Microhardness was measured using the Vickers method (HV1, 1 kgf), with at least three indentations performed at different locations for each sample.

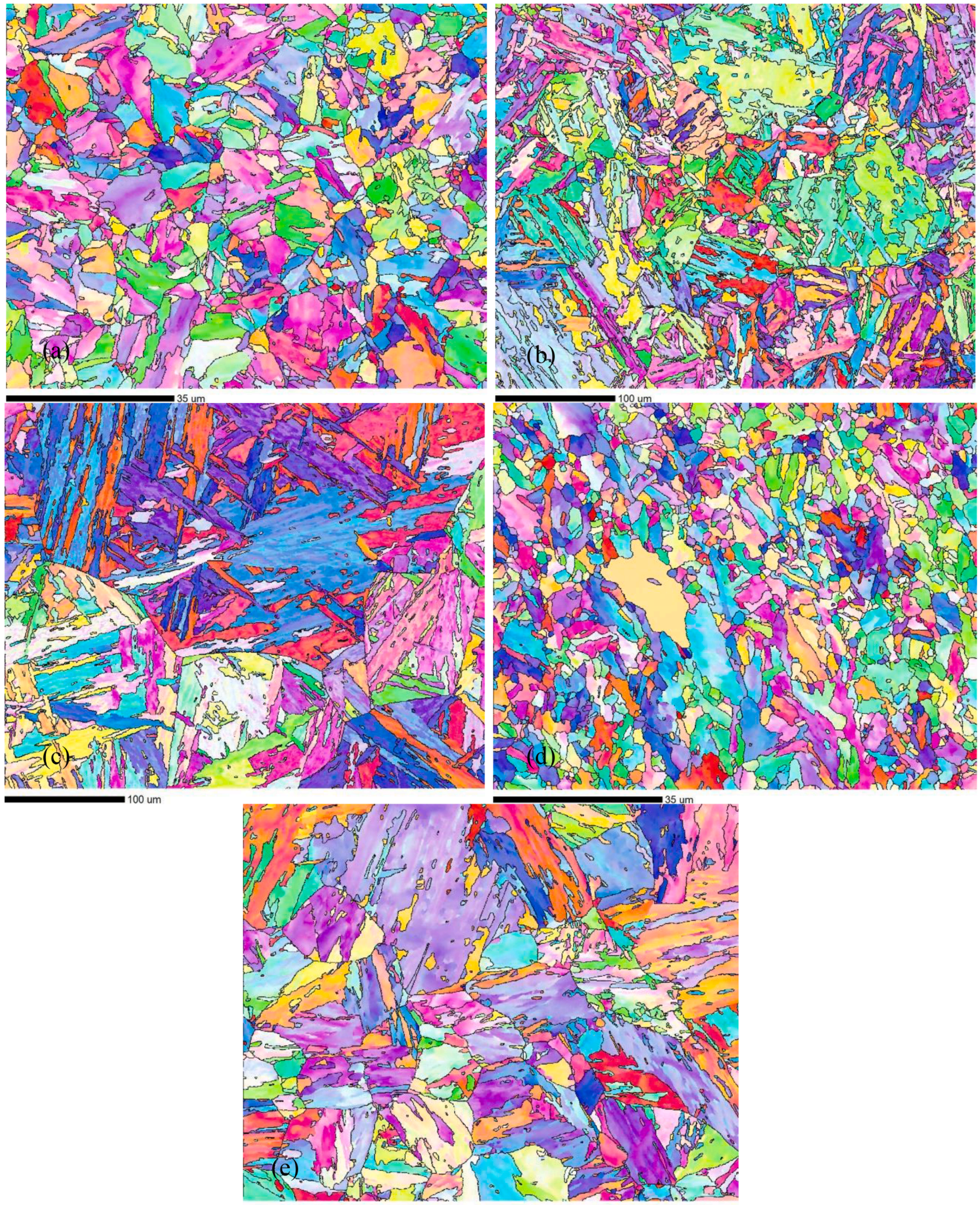

Fig. 2. EBSD maps of the RAFM steels in the unirradiated state: (a, b) EUROFER97 after different heat treatments: (a) 980 °C (0.5 h) AC + 780 °C (2 h) AC; (b) 1100 °C (0.5 h) AC + 700 °C (2 h) AC; (c) F82H: 960 °C (0.5 h) AC + 750 °C (1 h) AC; (d) M474: 880 °C (0.5 h) + 750 °C (2 h) AC; (e) L664B: 1000 °C (0.5 h) AC + 760 °C (1.5 h) AC. Field width: (a, d, e) 100 µm; (b, c) 400 µm.

Fig. 2 presents EBSD maps for all steels under investigation. The maps were acquired at two magnifications corresponding to fields of view of 100 µm (Fig. 2a, d, e) and 400 µm (Fig. 1b, c), since the sizes of prior austenite grains (PAGs) and martensitic packets strongly depend on the steel composition and the applied treatment. The grain (packet) sizes, evaluated both as number-weighted and area-weighted averages, are summarized in Table 8. In addition, PAG reconstruction was performed for all steels except M474, and the corresponding data are also included in Table 8.

All steels except M474 exhibit a typical tempered martensitic microstructure composed of lath and packet boundaries. In contrast, M474 shows a microstructure characteristic of a hot-rolled RAFM steel, consisting of more equiaxed ferritic grains. Along with fine grains, occasional larger grains with sizes up to ~20 µm are observed (Fig. 2d).

A pronounced effect of heat treatment on the microstructure is observed for EUROFER97-3. After the 980/780 heat treatment, the steel exhibits a significantly finer microstructure compared to the 1100/700 condition (Figs. 2a and b, respectively). The PAG size (area-weighted) after the 1100/700 heat treatment reaches ~80 µm, whereas after the 980/780 heat treatment, it is about ~9 µm. A similar trend is observed for the packet size: after the 980/780, the average packet size is approximately 5.2 µm, while after the 1100/700, it increases to about 16

Table 8
Packet size and prior austenite grain (PAG) size determined from EBSD analysis (area- and number-weighted averages), together with Vickers microhardness (HV1), for the RAFM steels in the unirradiated state.

Steel/Heat treatment	Packet size, µm		PAG size, µm		HV_1
	Area	Number	Area	Number	
EUROFER97-3_980 °C (0.5 h)/ 780 °C (2 h)	5.2	1.49	9.1	5.7	195-205
EUROFER97-3_1100 °C (0.5 h)/ 700 °C (2 h)	16	5.9	80	41	310-320
F82H_960 °C (0.5 h)/750 °C (1 h)	48	7.0	170	46	235-245
M474_880 °C (0.5 h)/750 °C (2 h)	4.3	1.64	-	-	205-215
L664B_1000 °C (0.5 h)/760 °C (1.5 h)	11.7	1.68	26	12	230-240

Table 9
Irradiation parameters for the RAFM steels tensile specimens.

Grade	T_{irr}, °C target/ actual	F, × 10^{26} m^{-2}, E > 0.1 MeV	D, dpa
EUROFER97-3_1100/700	325/330	4.96	22.1
	550/540	5.15	23.3
EUROFER97-3_980/780	325/330	4.67	20.8
	550/540	4.24	19.2
F82H	325/330	4.67	20.8
	550/540	4.82	21.8
M474	325/330	4.96	22.1
	550/540	5.26/4.24	23.8/19.2
L664B	325/330	4.96	22.1
	550/540	5.26/5.15	23.8/23.3

Table 10
Irradiation parameters for the RAFM steels Charpy impact specimens.

Grade	T_{irr}, °C target/ actual	F, × 10^{26} m^{-2}, E > 0.1 MeV	D, dpa
EUROFER97-3_1100/700	325/330	5.12	22.8
	550/540	4.77	21.6
EUROFER97-3_980/780	325/330	5.12	22.8
	550/540	4.77	21.6
F82H	550/540	5.26	23.8
M474	550/540	5.26	23.8
L664B	550/540	5.26	23.8

Table 11
Calculated duration of irradiation of the IR1a and IR2 rigs and the corresponding averaged fast neutron flux (E > 0.1 MeV).

Rig	T_{irr}, °C	F, × 10^{26} m^{-2}	t, day	θ, × 10^{19} $m^{-2}s^{-1}$
IR1a	330	4.67–4.96	516	1.05–1.11
IR2	540	5.15–5.26	434	1.37–1.40

µm. The coarsening of the microstructure in the latter case is attributed to the higher austenitization temperature.

F82H, despite undergoing a heat treatment similar to the lower-temperature EUROFER97-3 condition, exhibits the coarsest microstructure among the investigated steels (Fig. 2c). Although prior austenite grain (PAG) reconstruction was performed, the estimate is based on only a limited number of grains captured within the 400 µm field of view. Under these conditions, the PAG size reaches up to ~170 µm.

L664B (Fig. 2e) shows a packet size (number-weighted) similar to the EUROFER97-3 steel after the lower-temperature treatment, whereas the area-weighted packet size is somewhat larger.

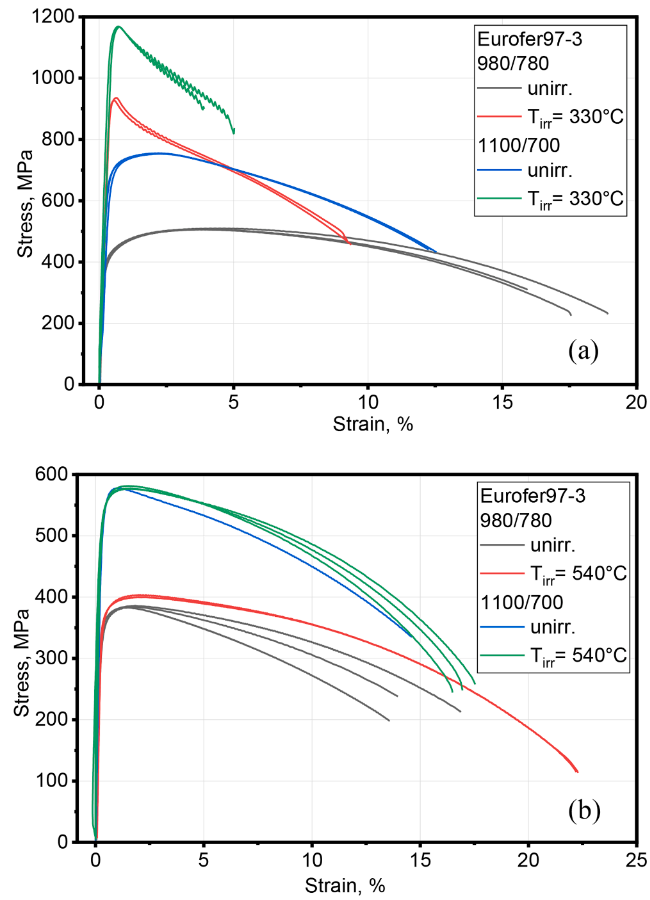

Fig. 3. The stress-strain diagrams of EUROFER97-3 before and after irradiation at 330 °C (a) and 540 °C (b) at testing temperature T_{test}=T_{irr}.

Overall, the EBSD maps confirm that the applied heat treatments result in predominantly homogeneous microstructures typical of RAFM steels, with no pronounced crystallographic texture at the examined scale.

Microhardness was measured using the Vickers method, and the results are summarized in Table 8. Overall, EUROFER97-3 in the lower-temperature heat-treated condition of 980/780 exhibits the lowest hardness, approximately 200 HV1. A slightly higher hardness is observed for M474, around 210 HV1. F82H and L664B show intermediate hardness values in the range of 230–240 HV1. In contrast, EUROFER97-3 in the higher-temperature heat-treated condition of 1100/700 exhibits the highest hardness, reaching approximately 315 HV1.

2.3. Irradiation

The EUROFER97-3, F82H, M474, L664B tensile and Charpy impact specimens were irradiated in the BOR-60 fast reactor, using the IR1a and IR2 rigs positioned in the 6th and 5th core rows, respectively, and contacted with sodium coolant during irradiation. The irradiation parameters for the tensile specimens are summarized in Table 9, and for the Charpy impact specimens are in Table 10. Table 11 shows additional irradiation parameters for the IR1a and IR2 rigs, such as the irradiation duration t and the average fast neutron flux θ. The averaging of the neutron flux was carried out due to the rearrangement of both rigs into different channels for the different reactor micro-runs, bearing in mind that each channel has its own specific fast neutron flux.

The specimens were housed in perforated capsules, allowing direct exposure to the circulating liquid sodium throughout irradiation. The specimen irradiation temperatures were determined from the

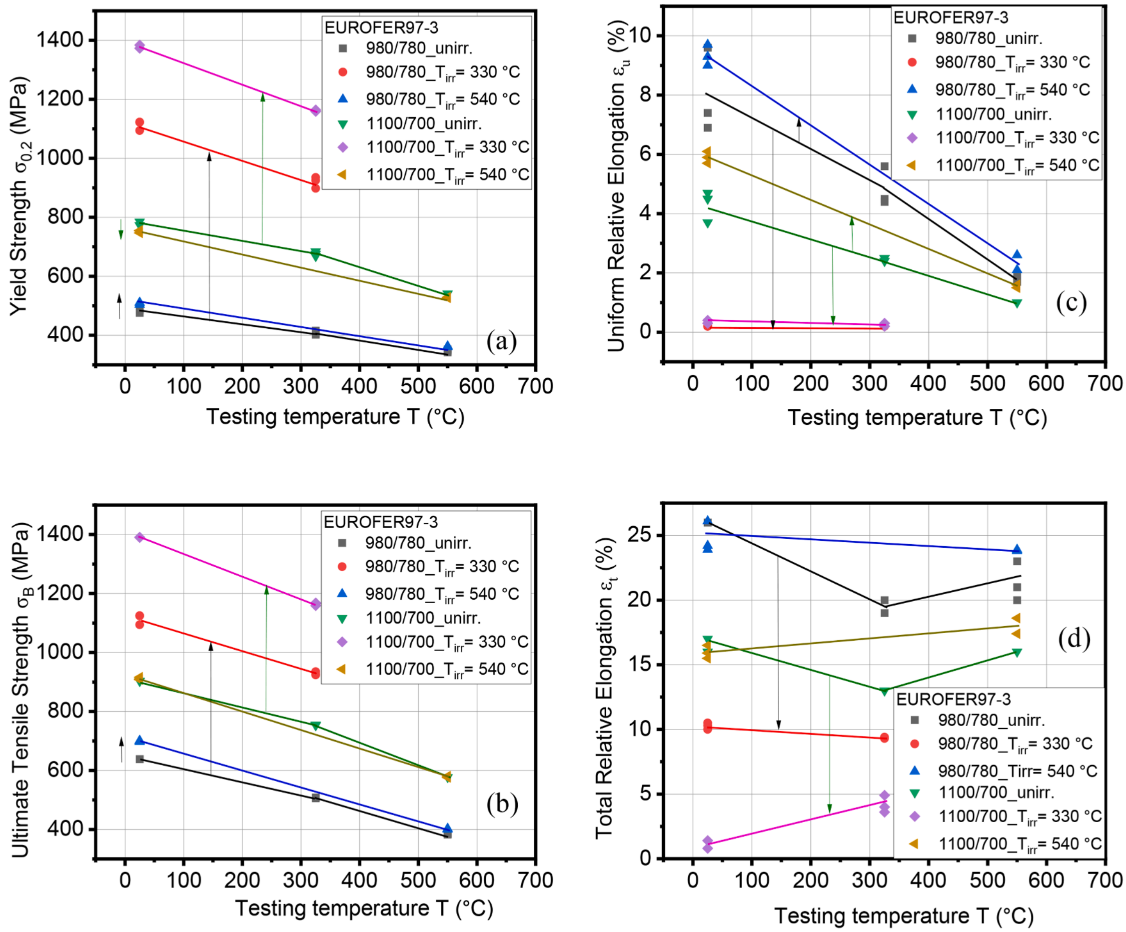

Fig. 4. Tensile properties of EUROFER97-3 before and after irradiation, irradiation temperature in °C: a) $\sigma_{0.2}$ vs. T; (b) σ_b vs. T; (c) ε_u vs. T; (d) ε_t vs. T where T, °C is testing temperature.

temperature of the sodium coolant flowing over them during reactor operation.

The irradiation conditions were evaluated using established data on energy deposition in the materials and on neutron flux levels within the reactor channels. The estimated accuracy of the temperature calculations is on the order of ±10 %, while neutron flux values carry an uncertainty of roughly ±20 %. The damage dose, computed for iron using the NRT (Norgett–Robinson–Torrens) methodology, was determined based on the precise axial positions of the tensile and Charpy impact specimens within the irradiation channels.

Both the IR1a and IR2 rigs were outfitted with temperature and neutron monitors, enabling tracking of irradiation parameters. These monitors were periodically removed for examination in a hot cell, after which replacement monitors were inserted to maintain ongoing surveillance.

As summarized in Tables 9 and 10, the actual irradiation temperatures and accumulated doses for the tensile and Charpy impact specimens stayed within the acceptable bounds relative to the specified target conditions.

2.4. Tensile testing

Testing of the tensile specimens before and after irradiation was conducted using the Zwick Universal Testing Machine (UTM) which was installed in a hot cell. The UTM is equipped with:

– high-temperature testing system with vacuum and a water-cooled inert gas chamber, along with a temperature controller that monitors and maintains the specimen temperature, recording temperature variations during testing;
– extensometer with ceramic probe tips, enabling instrumented testing in the temperature range from room temperature to 800 °C.

The RAFM steels specimens before and after irradiation were tested at a room temperature in air and at 325 °C and 550 °C in argon with the speed of testing actuator (grip) movement of 1 mm/min (strain rate 8.3 × 10^{-4} s^{-1}).

Three tensile specimens were tested at each test temperature however, not all tests were successful, the results of the unsuccessful tests were not included in this paper. From the load–displacement curves, strength and ductility properties including the 0.2 %-offset yield stress ($\sigma_{0.2}$), ultimate tensile strength (σ_B), uniform (ε_u) and total (ε_t) strain were determined. The margin of error for strength characteristics was ±5 %, while for strain it was ±10 %.

2.5. Charpy impact testing

The Mini-Charpy impact tests were performed in a hot-cell facility using an instrumented remote Zwick 5113 impact tester. The main specifications of the Zwick 5113 system are as follows:

- support span of 22 mm.
- a 15 J pendulum equipped with a 2-mm-radius instrumented striker;
- a temperature-conditioning unit capable of setting specimen temperatures between –190 and 680 °C;

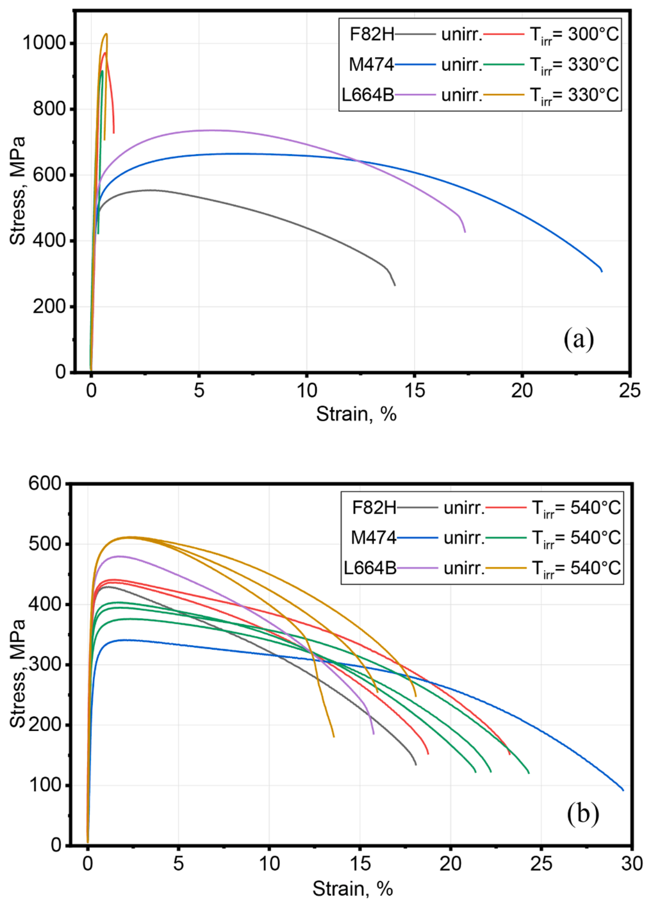

Fig. 5. Tensile properties of F82H, M474, L664B before and after irradiation,: a) $\sigma_{0.2}$ vs. T; (b) σ_b vs. T; (c) ε_u vs. T; (d) ε_t vs. T, where T, °C is the testing temperature.

- a pneumatic handling system that transfers specimens from the storage drum to the thermostat, and from the thermostat to the supports for testing.

During each test, the force–time curve was recorded, and the impact energy (fracture work) was obtained from this signal. The nominal test temperature reported in the protocol accounts for the actual temperature changes experienced by the specimen during transfer from the furnace to the supports and during hammer impact. The testing procedure follows the ISO-CD14556:2000(E) standard.

Following each test, the fractured specimen was visually examined with a webcam installed inside the hot cell.

3. Results

3.1. Tensile properties of EUROFER97-3 steel after irradiation at 330 °C and 540 °C

Fig. 3 shows the stress–strain diagrams for EUROFER97-3 of both heat treatments before and after irradiation at 330 °C (a) and 540 °C (b).

Fig. 4 presents the yield strength ($\sigma_{0.2}$) (Fig. 4a), ultimate tensile strength (σ_B) (Fig. 4b), and both the uniform (ε_u) (Fig. 4c) and total (ε_t) (Fig. 4d) elongations of EUROFER97-3 for both heat treatments before and after irradiation [8].

Prior to irradiation, EUROFER97-3_1100/700 exhibits higher strength accompanied by lower ductility, whereas EUROFER97-3_980/780 shows lower strength combined with higher ductility. A summary of the data in Fig. 4 reveals the following features of the radiation-induced evolution of the tensile properties of this steel.

Irradiation at 330 °C for both heat-treated variants of EUROFER97-3 leads to pronounced radiation hardening, as evidenced by a significant increase in both the yield and ultimate tensile strengths. At the same time, the uniform elongation decreases strongly below 1 %, while the total elongation remains in the range of 2–10 %.

In contrast, irradiation at 540 °C for both heat treatments results in only minor changes in yield and ultimate tensile strengths compared with the unirradiated condition. Both the uniform and total elongations remain stable, staying close to their pre-irradiation values.

Thus, the tensile test results for EUROFER97-3 with the two heat treatments irradiated up to 20 dpa demonstrate that irradiation temperature (330 °C versus 540 °C) has a markedly different impact on the mechanical behavior. At 330 °C, the tensile properties degrade significantly due to strong radiation-induced embrittlement, as indicated by the drastic reduction in uniform elongation. Conversely, at 540 °C, embrittlement effects are minimal: the steel largely retains its ductility and exhibits a modest increase in strength, which may be regarded as a positive effect.

3.2. Tensile properties of F82H, M474, L664B steels after irradiation at 330 °C and 540 °C

Fig. 5 shows the stress–strain diagrams for F82H, M474 and L664B steels before and after irradiation at 330 °C (a) and 540 °C (b).

Fig. 6 presents the yield strength ($\sigma_{0.2}$) (Fig. 6a), ultimate tensile strength (σ_B) (Fig. 6b), and both the uniform (ε_u) (Fig. 6c) and total (ε_t) (Fig. 6d) elongations of the F82H, M474, and L664B RAFM steels before and after irradiation. Prior to irradiation, these steels exhibit similar tensile properties, with only minor differences in strength and ductility.

Overall, these steels show tensile behavior comparable to that of EUROFER97-3, even after irradiation. Specifically, after irradiation at 330 °C and testing at 325 °C, all three steels exhibit a pronounced increase in yield and ultimate tensile strengths, accompanied by a strong reduction in uniform elongation to values below 1 %. However, the total elongation remains above approximately 5–10 %.

Similar to EUROFER97-3, the tensile properties of these steels change only slightly after irradiation at 540 °C and testing at 550 °C. At this irradiation temperature, only a modest increase in strength is observed, while the plastic tensile properties of all three steels remain close to their pre-irradiation values.

3.3. Charpy impact properties of EUROFER97-3 after irradiation at 330 °C and 540 °C

Fig. 7 shows the impact energy (A_v) as a function of test temperature (T_{test}) for EUROFER97-3_1100/700 (Fig. 7a) and EUROFER97-3_980/780 (Fig. 7b) in unirradiated conditions and after irradiation at 330 °C and 540 °C, respectively [9]. The curves in Fig. 7 result from the sigmoid (logistic/Boltzmann) approximation (nonlinear fit) to the experimental data points as follows:

$$E(T) = E_{low} + \left(E_{high} - E_{low}\right)/(1 + \exp(-(T - T_0)/k)), \quad (1)$$

where E_{low}, J is the asymptotic value of the lower shelf energy (LSE); E_{high}, J is the asymptotic value of the upper shelf energy (USE); T_0, K is the test temperature; T, K is a current temperature under approximation process.

In unirradiated conditions, the two heat-treated variants of EUROFER97-3 exhibit distinctly different impact properties. EUROFER97-3_1100/700 shows a lower USE (8.5 J vs. 10.4 J) and a significantly higher ductile-to-brittle transition temperature (DBTT) (−8 °C vs. −121 °C) compared with EUROFER97-3_980/780 (see Table 12).

Neutron irradiation degrades the Charpy impact properties of both heat-treated variants, resulting in a reduction in the USE and an increase of the DBTT. However, the magnitude of the irradiation-induced changes depends on both the heat treatment of EUROFER97-3 and the

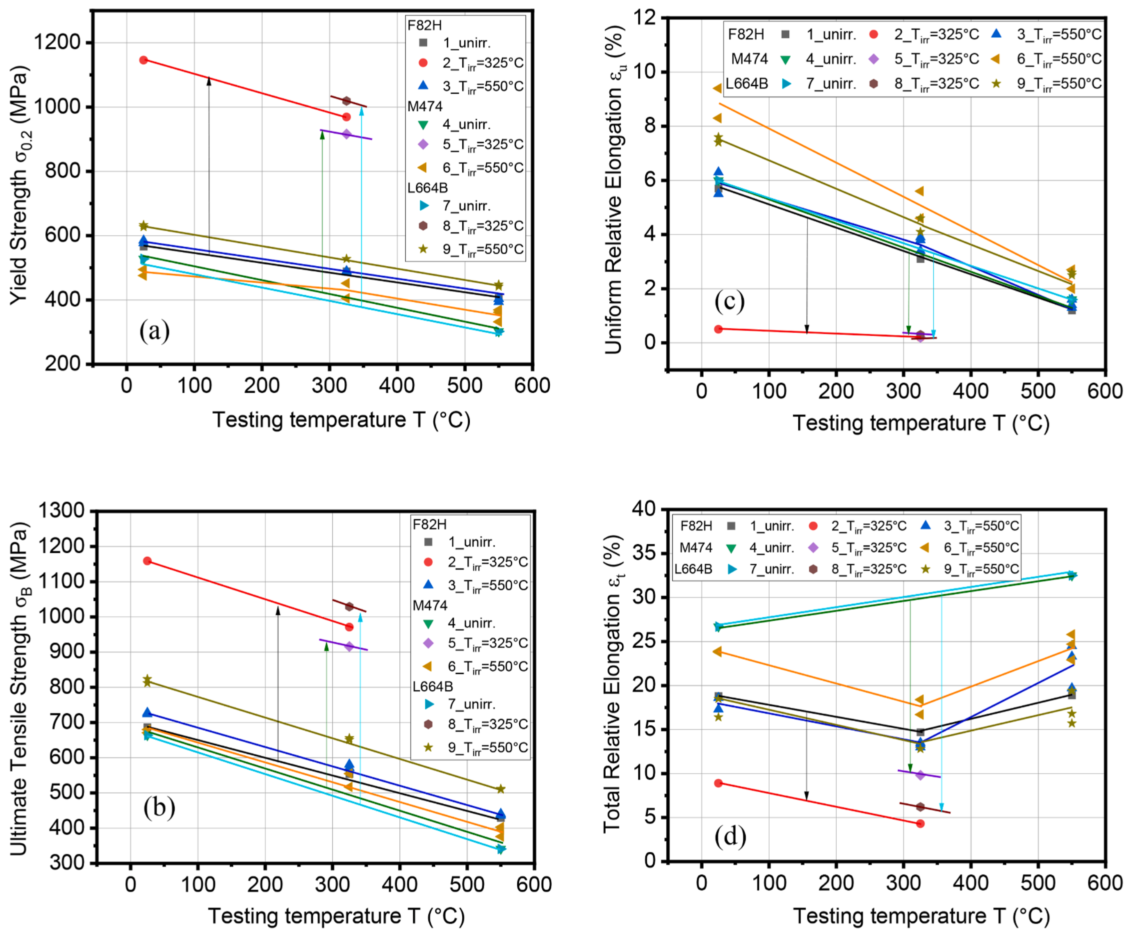

Fig. 6. Tensile properties of F82H, M474, L664B before and after irradiation,: a) $\sigma_{0.2}$ vs. T; (b) σ_b vs. T; (c) ε_u vs. T; (d) ε_t vs. T, where T, °C is the testing temperature.

irradiation temperature.

Irradiation at 330 °C leads to a pronounced decrease in the USE and an increase of the DBTT for EUROFER97-3 in both heat-treated conditions. However, the detrimental effect of irradiation is much more severe for EUROFER97-3_1100/700 than for EUROFER97-3_980/780 (see Table 12). Post-irradiation annealing at 550 °C for 4 h results in a partial recovery of the impact properties of EUROFER97-3_1100/700, as is indicated by an increase in the USE and a reduced DBTT.

In contrast, irradiation at 540 °C has a substantially smaller effect on the Charpy impact properties of EUROFER97-3. After irradiation, the impact properties deteriorate only slightly: the USE for both heat treatments decreases by no >10–13 %, and the DBTT increases only for 1 °C for EUROFER97-3_1100/700 and for 30 °C for EUROFER97-3_980/780, respectively (see Table 12).

In summary, for EUROFER97-3 in both heat-treated conditions, irradiation up to 20 dpa results in markedly different radiation-induced effects on Charpy impact properties depending on the irradiation temperature. At 330 °C, the degradation of impact properties is much more pronounced, whereas at 540 °C the irradiation-induced effects are minimal.

3.4. Charpy impact properties of F82H, M474, and L664B steels after irradiation at 540 °C

Fig. 8 presents the Charpy impact properties of three RAFM steels before and after irradiation at 540 °C up to 20 dpa. The results obtained from the analysis of the impact energy vs. temperature diagrams are summarized in Table 12.

Prior to irradiation, M474 exhibits the lowest DBTT at −90 °C, whereas the other two steels, F82H and L664B, have similar DBTT values of −30 °C and −20 °C, respectively. After irradiation at 540 °C, M474 still retains the lowest DBTT (−40 °C), L664B shows the highest DBTT (30 °C), and F82H exhibits an intermediate value (−10 °C).

Prior to irradiation, M474 exhibits the highest upper-shelf energy (USE) at 10.3 J, while the other two steels show lower USE values. After irradiation, M474 also demonstrates the smallest reduction in the USE.

Overall, it can be concluded that despite some differences in the magnitude of the radiation-induced effect, irradiation at 540 °C has a relatively minor and non-critical influence on the Charpy impact properties of these three RAFM steels.

4. Discussion

4.1. Comparison of tensile properties

Fig. 9 illustrates the increase in yield strength, $\Delta\sigma_{0.2} = \sigma_{0.2\ irr} - \sigma_{0.2\ unirr}$, for all steels investigated after irradiation at two different temperatures, which represents the radiation-induced hardening. As clearly shown, the extent of radiation hardening differs markedly between irradiation at 330 °C and at 540 °C.

After irradiation at 330 °C, $\Delta\sigma_{0.2}$ increases sharply to approximately 400–500 MPa, whereas after irradiation at 540 °C it is close to zero and does not exceed 150 MPa for the L664B steel.

When comparing the steels, no significant differences in radiation hardening are observed among them at a given irradiation temperature.

Fig. 10 shows the radiation-induced change in uniform elongation, $\Delta\varepsilon_u = \varepsilon_{u\ irr} - \varepsilon_{u\ unirr}$, for two irradiation temperatures. As in the case of radiation hardening, a pronounced difference in the effect on uniform

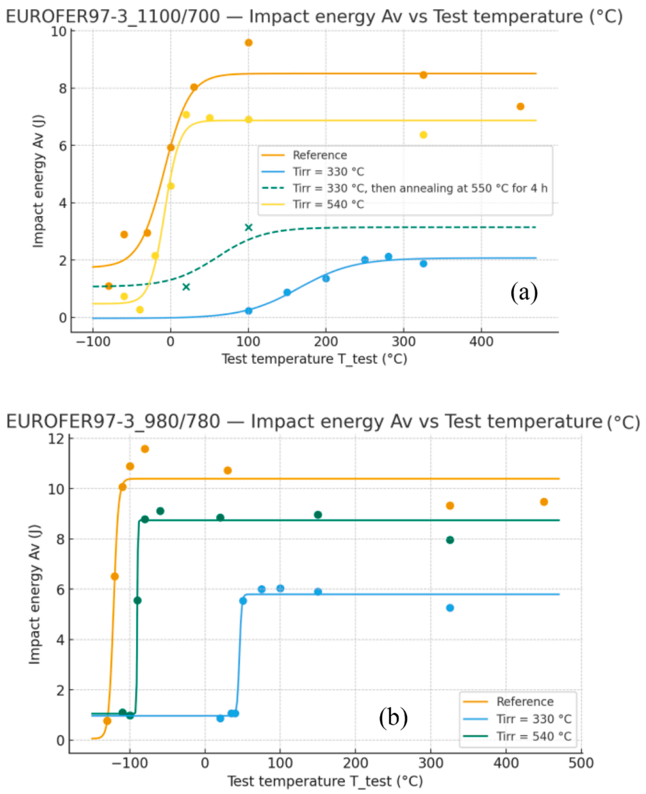

Fig. 7. Impact energy A_v vs. Test Temperature T for EUROFER97-3_1100/700 (a) and EUROFER97-3_980/780 (b) before and after irradiation.

Table 12
Results of processing of A – T diagrams for EUROFER97-3_980/780, EUROFER97-3_1100/700, F82H, M474, and L664B RAFM steels before (unirr.) and after (irr.) irradiation at 540 °C.

Steel/Heat treatment	State	Upper-shelf energy (USE), J	Lower shelf energy (LSE), J	DBTT, °C
EUROFER97-3_1100/700	unirr.	8.5	1.7	−8
EUROFER97-3_1100/700	irr.	6.9	0.5	−7
EUROFER97-3_980/780	unirr.	10.4	0.1	−121
EUROFER97-3_980/780	irr.	8.7	1.1	−90
F82H	unirr.	7.6	0.4	−30
F82H	irr.	7.0	0.2	−10
M474	unirr.	10.3	0.3	−90
M474	irr.	9.6	0.4	−40
L664B	unirr.	6.7	0.6	−20
L664B	irr.	5.0	1.2	30

elongation is observed between the two irradiation temperatures, but in the opposite sense. At 540 °C, the change in uniform elongation is minimal, remaining within ±1 % for all steels, whereas at 330 °C the reduction is much more substantial, ranging from −2 % to −6 %.

A notable feature of EUROFER97-3_1100/700 is that it exhibits a comparatively large decrease in uniform elongation at 540 °C and a relatively small decrease at 330 °C.

There is no literature data available on radiation-induced hardening of RAFM steels after irradiation at high temperatures such as 540 °C. For irradiation at 330 °C, however, the reported radiation hardening of EUROFER97 irradiated at 300–335 °C up to approximately 30 dpa is about 500 MPa [12], which is in good agreement with the results shown in Fig. 9.

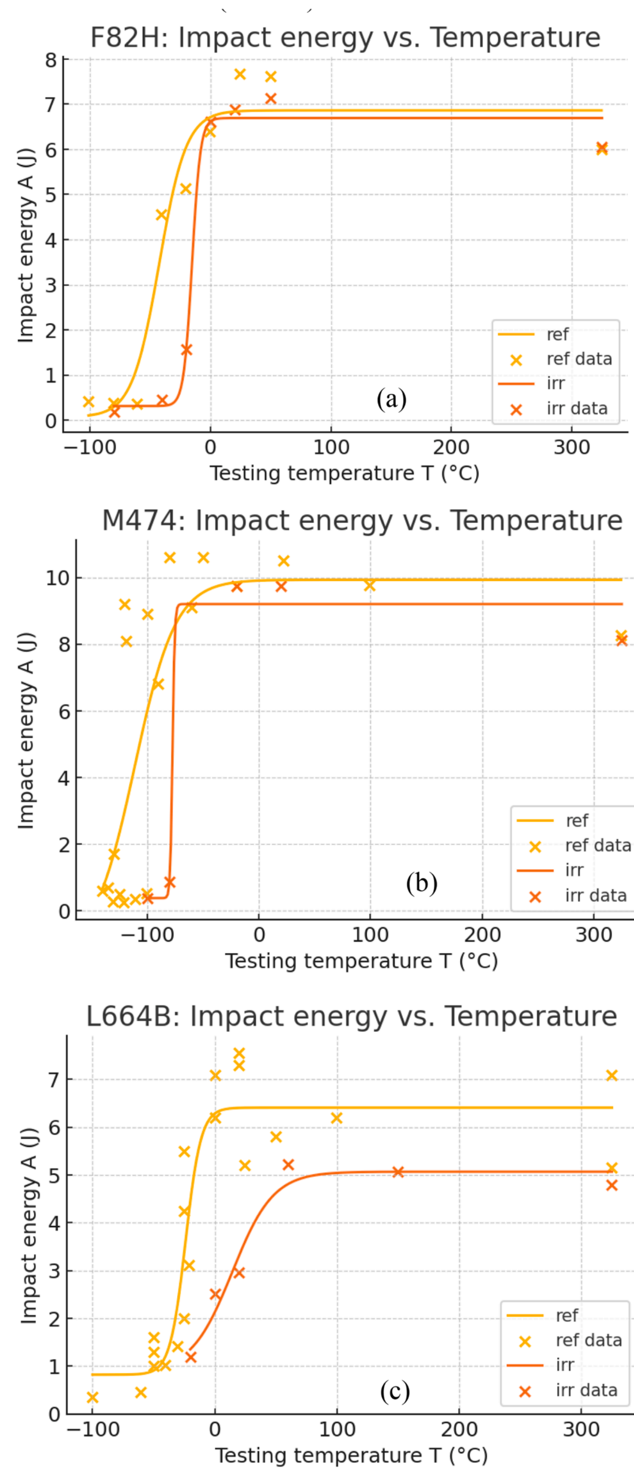

Fig. 8. Impact energy A – Temperature T diagrams for M474 (a), L664B (b), F82H (c) steels before (ref) and after (irr) irradiation.

4.2. Comparison of Charpy impact properties

4.2.1. EUROFER97-3, T_{irr}= 330 °C and 540 °C

In the literature [11–16], only a limited number of Charpy impact test results are available for EUROFER97 and other RAFM steels after neutron irradiation under fusion relevant conditions. Among these, the most representative study is Ref. [11], in which Gaganidze reports Charpy impact test results for RAFM steels, including EUROFER97 batch 1 after irradiation in the BOR-60 fast reactor at 330–340 °C up to 70 dpa.

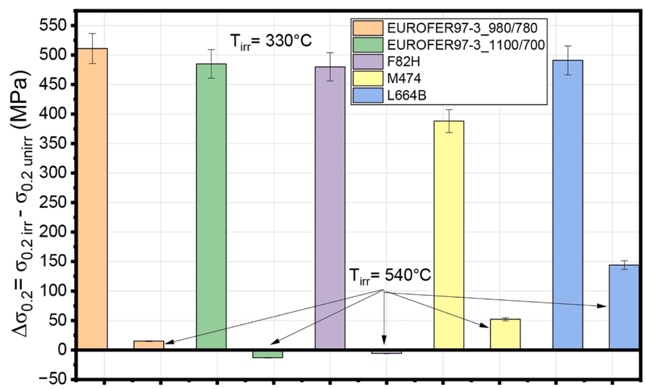

Fig. 9. Radiation-induced hardening $\Delta\sigma_{0.2} = \sigma_{0.2\ irr} - \sigma_{0.2\ unirr}$ of RAFM steels such as EUROFER97-3_980/780, EUROFER97-3_1100/700, F82H, M474 and L664B after irradiation at 330 °C (T_{test} = 325 °C) and 540 °C (T_{test} = 550 °C) up to 19–24 dpa. For M474 and L664B, there is no data for unirradiated state at T_{test} = 325 °C therefore, instead of this temperature, the tests at room temperature (see Figs. 5a and 6a) were taken.

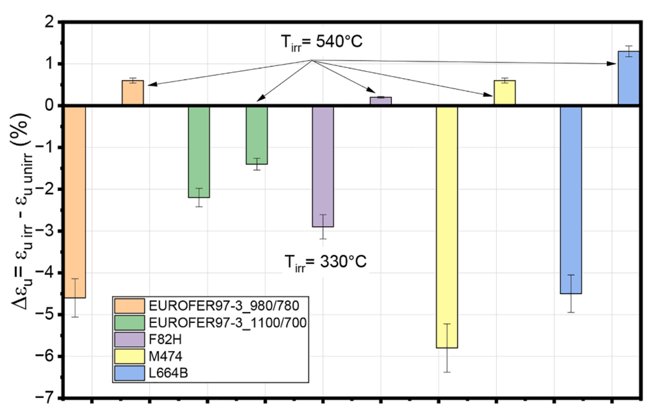

Fig. 10. Radiation-induced decrease of uniform relative elongation $\Delta\varepsilon_u = \varepsilon_{u\ irr} - \varepsilon_{u\ unirr}$ of RAFM steels such as EUROFER97-3_980/780, EUROFER97-3_1100/700, F82H_960/750, M474 and L664B_1000/750 after irradiation at 330 °C (T_{test} = 325 °C) and 540 °C (T_{test} = 550 °C) up to 19–24 dpa. For M474 and L664B, there is no data for unirradiated state at T_{test} = 325 °C therefore, instead of this temperature, the tests at room temperature (see Fig. 5a, 6c) were taken.

Fig. 11 presents a comparison of the decrease in upper-shelf energy (USE) obtained in the present study. A pronounced degradation of the USE is observed for both heat-treated variants of EUROFER97-3 after irradiation at 330 °C (Fig. 11a). A larger reduction in the USE occurred for EUROFER97-3_1100/700 than for EUROFER97-3_980/780 (Fig. 11b). Short-term annealing at 550 °C for 4 h led to a partial recovery of the USE in EUROFER97-3_1100/700. This observation is consistent with the well-known approach for restoring the plasticity of irradiated bcc metals and alloys through short-term annealing at elevated temperatures, including EUROFER97 [12,13].

Fig. 11b shows the shift in the ductile-to-brittle transition temperature (DBTT) for EUROFER97-3_980/780 and EUROFER97-3_1100/700 after irradiation at 330 °C and 540 °C. The behavior of ΔDBTT correlates with the USE results: a pronounced shift occurs after irradiation at 330 °C, with partial recovery following short-term annealing at 550 °C, whereas only a minimal shift in the DBTT is observed after irradiation at 540 °C.

Gaganidze et al. [12] provides data on the radiation behavior of EUROFER97 batch 1. For example, steels with very similar heat treatment (980/780 in the present study and 980/760 in [11]) were irradiated up to about 70 dpa. Despite the difference in the damage doses of about factor three, the USE for both irradiated materials is approximately the same, around 6 J. However, the higher dose results in a larger shift in the DBTT (ΔDBTT~150 °C versus ~50 °C).

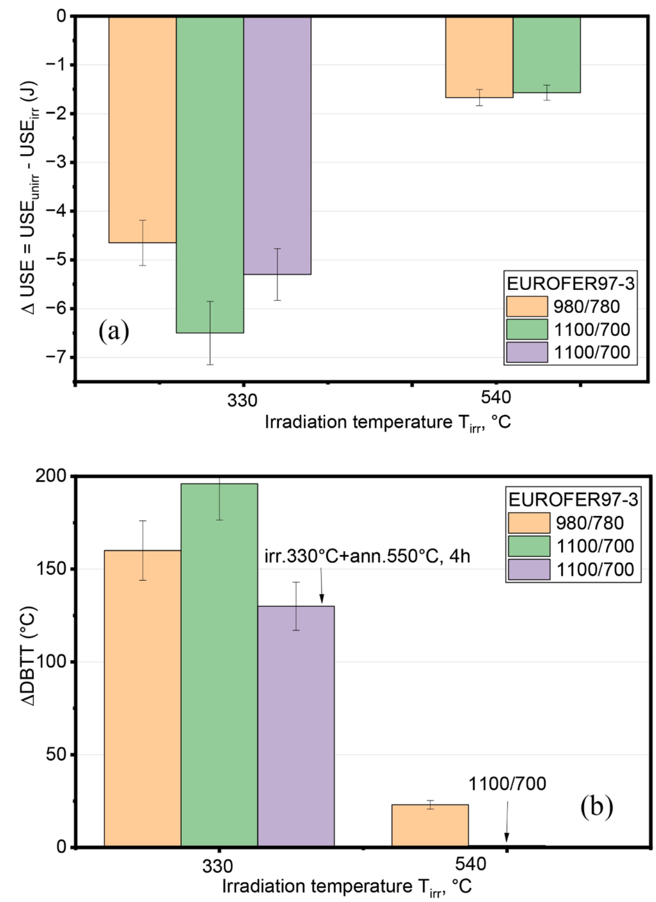

Fig. 11. Radiation-induced decrease of the USE (a) and shift of the DBTT (b) of EUROFER97-3_980/780 and EUROFER97-3_1100/700 after irradiation at 330 °C and 540 °C up to ~20 dpa.

There is a complete lack of literature data on the Charpy impact properties of EUROFER97 steel after irradiation at 540 °C. Irradiation of the EUROFER97_ANL state in the HFR at 400 °C and 450 °C up to 16.3 dpa leads to only a slight shift in the DBTT and a small decrease in the USE [12–17]. This is consistent with the results of the present study, although our irradiation temperature was higher (540 °C versus 450 °C).

Currently, EUROFER97-3_980/780 is irradiated up to a damage dose of 40 dpa, with impact testing of the irradiated specimens planned for mid-2026. Based on available literature data [12], the DBTT in this case is expected to be in the range of 50–150 °C.

4.2.2. *EUROFER97-3, F82H, M474, and L664B,*

T_{irr} = 540°C

Fig. 12 presents a comparison of the Charpy impact properties of all RAFM steels that were investigated in the present study, irradiated in the BOR-60 fast reactor at 540 °C up to a damage dose of ~20 dpa. Figs. 12a and 12b illustrate the respective shifts of the DBTT.

It can be seen that EUROFER97-3_980/780 and M474 steels exhibit the lowest DBTT values. However, when comparing the ΔDBTT between these two steels, EUROFER97-3_980/780 shows a smaller shift than M474 (22 °C versus 50 °C).

Fig. 12c shows the behavior of the USE, from which it follows that EUROFER97-3_980/780 and M474 have the highest USE both before and after irradiation states. Overall, however, none of the steels studied exhibited significant changes in their Charpy impact properties (DBTT

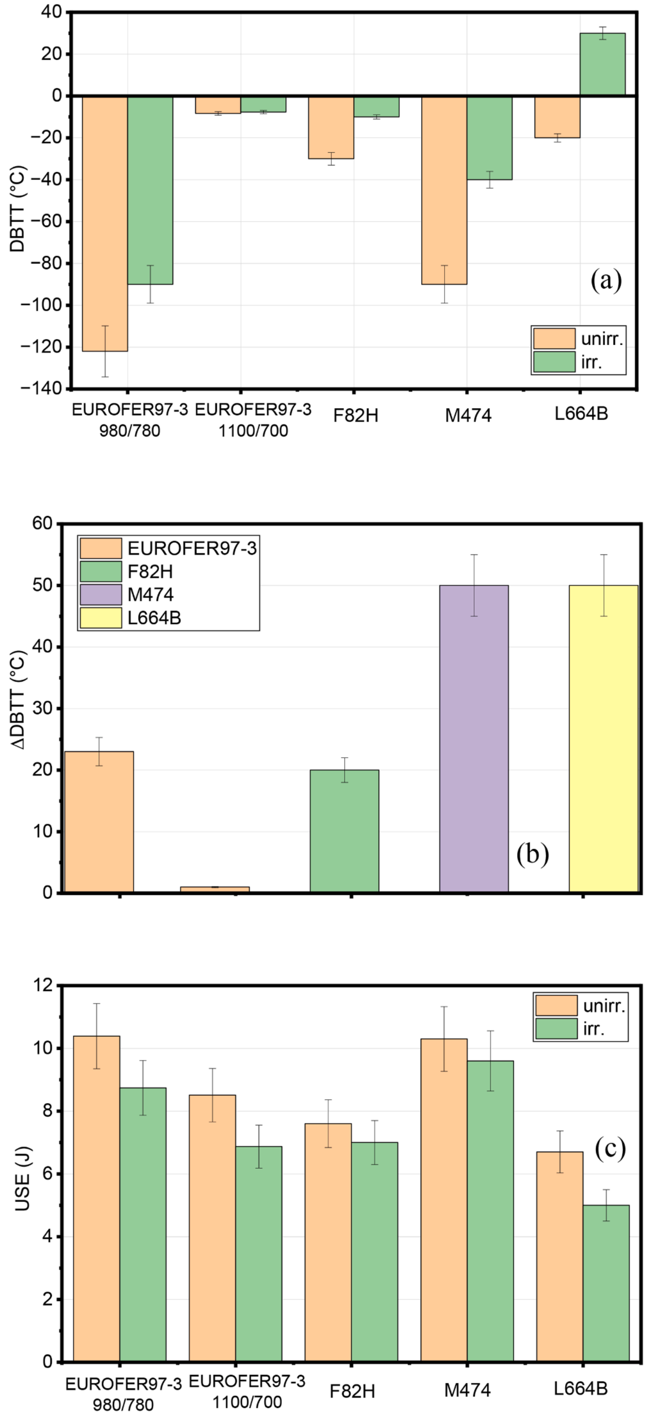

Fig. 12. Comparison of DBTT (a), ΔDBTT (b) and USE (c) for EUROFER97-3_980/780, EUROFER97-3_1100/700, F82H, M474 and L664B RAFM steels before and after irradiation at T_{irr}= 540 °C.

or USE) after irradiation at 540 °C, indicating that their behavior is generally similar.

Fracture surface studies of the impact-tested specimens irradiated at 330 °C and 540 °C to ~20 dpa are scheduled for the first half of 2026. These studies will provide insights into the radiation-induced microstructural features of EUROFER97-3, allowing a deeper understanding of the Charpy impact property (as well as tensile one) results reported in this study [18–21].

The difference in irradiation temperatures leads to a fundamental change in how neutron irradiation affects the tensile and Charpy impact properties of the RAFM steels investigated in this study. At an irradiation temperature of 330 °C, as reported in the literature [12], dislocation loops form, resulting in pronounced radiation hardening and, consequently, embrittlement of the steels.

At 540 °C, however, in-situ annealing during irradiation becomes significant. Since no data are currently available in the literature on the microstructural evolution of RAFM steels irradiated at such a high temperature, definitive conclusions cannot yet be drawn without direct TEM investigations. Nevertheless, it is reasonable to assume that annealing processes during irradiation suppress the formation of dislocation loops and other radiation-induced defects, unlike at the comparatively lower temperature of 330 °C. It therefore appears that the phase structure of RAFM steels irradiated at 540 °C does not undergo substantial changes. As a result, their mechanical properties do not degrade to the same extent as at 330 °C.

This behavior can be attributed to two main factors: (i) the absence or reduced density of dislocation loops and other radiation defects due to their annealing during irradiation, and (ii) the absence or reduced possible modifications in the composition and morphology of pre-existing phases. These assumptions will be rigorously validated through forthcoming TEM studies of these RAFM steels irradiated at 330 °C and 540 °C up to 20 dpa, which are planned to be completed by mid-2026.

5. Conclusions

The tensile and Charpy impact properties of EUROFER97-3_980/780, EUROFER97-3_1100/700, F82H, M474, and L664B RAFM steels were investigated before and after irradiation in the BOR-60 fast reactor at actual average temperatures of 330 °C and 540 °C, respectively. The damage doses in this study ranged from 19.2 to 23.8 dpa.

The main findings are as follows:

Tensile properties.

- At 330 °C, irradiation induces strong hardening in all investigated steels, resulting in a pronounced increase in both yield and ultimate tensile strengths. This is accompanied by a sharp decrease in uniform elongation to less than 1 %, while the total elongation remains in the range of 2–10 %.
- At 540 °C, irradiation causes only minor changes in yield and ultimate tensile strengths, as well as in both uniform and total elongations in all investigated steels.

Charpy impact properties.

- At 330 °C, irradiation causes substantial degradation of the Charpy impact properties of EUROFER97-3 for both heat treatments, characterized by a marked decrease in USE and a significant increase of DBTT. EUROFER97-3_980/780 exhibits less degradation than the state EUROFER97-3_1100/700. Short-term annealing (550 °C for 4 h) after irradiation at 330 °C partially restores the Charpy impact properties of EUROFER97-3_1100/700.
- At 540 °C, irradiation causes only minor changes in the Charpy impact properties of EUROFER97-3 (both heat treatments) as well as F82H, M474, and L664B RAFM steels.

General remarks.

- The pronounced difference in the overall response of the studied steels to irradiation at 330 °C and 540 °C, a temperature difference of only 210 °C, warrants detailed investigation using microstructural techniques (SEM, TEM) and subsequent analysis to explain the observed behavior.
- Nevertheless, it can already be concluded that the minimal effect of irradiation at the high temperature of 540 °C up to 20 dpa, observed here for the first time in RAFM steels, indicates the absence of critical

changes in tensile strength, ductility, and Charpy impact properties (ΔUSE and ΔDBTT).

CRediT authorship contribution statement

Vladimir Chakin: Writing – review & editing, Writing – original draft, Supervision, Methodology, Investigation, Formal analysis. **Carsten Bonnekoh:** Writing – review & editing, Supervision, Software, Methodology, Investigation. **Ramil Gaisin:** Writing – review & editing, Software, Methodology, Investigation, Formal analysis. **Rainer Ziegler:** Writing – review & editing, Validation, Investigation. **Michael Duerrschnabel:** Writing – review & editing, Software, Methodology, Investigation. **Michael Klimenkov:** Writing – review & editing, Methodology, Investigation, Formal analysis, Data curation. **Hans-Christian Schneider:** Writing – review & editing, Visualization, Supervision, Investigation. **Rolf Rolli:** Writing – review & editing, Investigation, Data curation. **Bronislava Gorr:** Writing – review & editing, Resources, Project administration, Conceptualization. **Michael Rieth:** Writing – review & editing, Supervision, Resources, Project administration, Funding acquisition, Data curation, Conceptualization. **Dmitry Terentyev:** Writing – review & editing, Investigation, Conceptualization. **Jean Henry:** Writing – review & editing, Investigation, Conceptualization. **Takashi Nozawa:** Writing – review & editing, Methodology, Investigation, Conceptualization.

Declaration of competing interest

The authors declare that they have no known competing financial interests or personal relationships that could have appeared to influence the work reported in this paper.

Acknowledgements

This work has been carried out within the framework of the EUROfusion Consortium, funded by the European Union via the Euratom Research and Training Programme (Grant Agreement No 101052200 — EUROfusion). Views and opinions expressed are, however, those of the authors only and do not necessarily reflect those of the European Union or the European Commission. Neither the European Union nor the European Commission can be held responsible for them.

This work was partly supported by the R&D on Development of Structural Material for Fusion DEMO In-Vessel Components in Phase II for the DEMO R&D for the IFERC Project.

We would like to express our sincere gratitude to the staff of the Research Institute of Atomic Reactors for their organization of the irradiation and post-irradiation examinations of the materials, as well as for the insightful and fruitful discussions regarding the results obtained in this study.

We also thank Dr. Thomas Bergfeldt for the chemical analysis of the EUROFER97-3 steel and Daniel Bolich for performing heat treatments and preparation of the specimens for microstructure studies.

Data availability

No data was used for the research described in the article.

References

[1] M. Rieth, M. Dürrschnabel, S. Bonk, U. Jäntsch, T. Bergfeldt, J. Hoffmann, S. Antusch, E. Simondon, M. Klimenkov, C. Bonnekoh, B. Ghidersa, H. Neuberger, J. Rey, C. Zeile, G. Pintsuk, G. Aiello, Technological processes for steel applications in nuclear fusion, Appl. Sci. 11 (2021) 11653, https://doi.org/10.3390/app112411653.
[2] M. Rieth, M. Dürrschnabel, S. Bonk, S. Antusch, G. Pintsuk, G. Aiello, J. Henry, Y. de Carlan, B.-E. Ghidersa, H. Neuberger, et al., Fabrication routes for advanced first wall design alternatives, Nucl. Fusion 61 (2021) 116067.
[3] G. Federici, C. Bachmann, L. Barucca, W. Biel, L. Boccaccini, R. Brown, C. Bustreo, S. Ciattaglia, F. Cismondi, M. Coleman, V. Corato, C. Day, E. Diegele, U. Fischer, T. Franke, C. Gliss, A. Ibarra, R. Kembleton, A. Loving, F. Maviglia, B. Meszaros, G. Pintsuk, N. Taylor, M.Q. Tran, C. Vorpahl, R. Wenninger, J.H. You, DEMO design activity in Europe: progress and updates, Fusion Eng. Des. 136 (2018) 729–741.
[4] G. Federici, L. Boccaccini, F. Cismondi, M. Gasparotto, Y. Poitevin, I. Ricapito, An overview of the EU breeding blanket design strategy as an integral part of the DEMO design effort, Fusion Eng. Des. 141 (2019) 30–42.
[5] F.A. Hernández, P. Pereslavtsev, G. Zhou, Q. Kang, S. D'Amico, H. Neuberger, L. V. Boccaccini, B. Kiss, G. Nádasi, L. Maqueda, I. Cristescu, I. Moscato, I. Ricapito, F. Cismondi, Consolidated design of the HCPB breeding blanket for the pre-conceptual design phase of the EU DEMO and harmonization with the ITER HCPB TBM program, Fusion Eng. Des. 157 (2020) 111614.
[6] M. Duerrschnabel, U. Jaentsch, R. Gaisin, M. Rieth, Microstructural insights into EUROFER97 batch 3 steels, Nucl. Mater. Energy 35 (2023) 101445.
[7] A.L. Izhutov, Y.M. Krasheninnikov, I.Y. Zhemkov, A.V. Varivtsev, Y. V. Naboischikov, V.S. Neustroev, V.K. Shamardin, Prolongation of the BOR-60 reactor operation, Nucl. Eng. Techn. 47 (3) (2015) 253–259.
[8] V. Chakin, C. Bonnekoh, R. Gaisin, R. Ziegler, M. Duerrschnabel, M. Klimenkov, B. Gorr, M. Rieth, Tensile properties of EUROFER97-3 after neutron irradiation at 330 °C and 540 °C to damage doses of 19–23 dpa, Nucl. Mater. Energy 45 (2025) 102034.
[9] V. Chakin, C. Bonnekoh, R. Gaisin, R. Ziegler, M. Duerrschnabel, M. Klimenkov, B. Gorr, M. Rieth, Impact bending properties of EUROFER97-3 after neutron irradiation at 330 °C and 540 °C to damage doses of 21-23 dpa, Nucl. Mater. Energy (2026) under review.
[10] V. Chakin, C. Bonnekoh, R. Ziegler, R. Gaisin, M. Duerrschnabel, M. Klimenkov, M. Rieth, B. Gorr, M. Toloczko, Creep behavior of EUROFER97–3 steel during neutron irradiation at 325°C and 550°C to 7–24 dpa, Fusion Eng. Des. 215 (2025) 115014.
[11] D. Terentyev, O. Kachko, A. Puype, S. Valiyev, K. Iroc, A. Zinovev, Development of irradiation- and high-temperature resistant steels for fusion applications: Belgian contribution, J. Nucl. Mater. 606 (2025) 155611.
[12] E. Gaganidze, C. Petersen, E. Materna-Morris, C. Dethloff, O.J. Weiß, J. Aktaa, A. Povstyanko, A. Fedoseev, O. Makarov, V. Prokhorov, Mechanical properties and TEM examination of RAFM steels irradiated up to 70 dpa in BOR-60, J. Nucl. Mater. 417 (2011) 93–98.
[13] C. Petersen, A. Povstyanko, V. Prokhorov, A. Fedoseev, O. Makarov, B. Dafferner, Impact property degradation of ferritic/martensitic steels after the fast reactor irradiation 'ARBOR 1', J. Nucl. Mater. 367–370 (2007) 544–549.
[14] E. Gaganidze, H.-C. Schneider, B. Dafferner, J. Aktaa, Embrittlement behavior of neutron irradiated RAFM steels, J. Nucl. Mater. 367–370 (2007) 81–85.
[15] E. Gaganidze, J. Aktaa, The effects of helium on the embrittlement and hardening of boron doped EUROFER97 steels, Fusion Eng. Des. 83 (2008) 1498–1502.
[16] B. van der Schaaf, C. Petersen, Y. De Carlan, J.W. Rensman, E. Gaganidze, X. Averty, High dose, up to 80 dpa, mechanical properties of Eurofer 97, J. Nucl. Mater. 386–388 (2009) 236–240.
[17] C. Cabet, F. Dalle, E. Gaganidze, J. Henry, H. Tanigawa, Ferritic-martensitic steels for fission and fusion applications, J. Nucl. Mater. 523 (2019) 510–537.
[18] M. Klimenkov, U. Jeantsch, M. Rieth, A. Moeslang, Correlation of microstructural and mechanical properties of neutron irradiated EUROFER97 steel, J. Nucl. Mater. 538 (2020) 152231.
[19] M. Klimenkov, U. Jäntsch, M. Rieth, M. Dürrschnabel, A. Möslang, H.C. Schneider, Post-irradiation microstructural examination of EUROFER-ODS steel irradiated at 300°C and 400°C, J. Nucl. Mater. 557 (2021) 153259.
[20] M. Klimenkov, A. Möslang, E. Materna-Morris, Helium influence on the microstructure and swelling of 9%Cr ferritic steel after neutron irradiation to 16.3 dpa, J. Nucl. Mater. 453 (2014) 54–59.
[21] M. Klimenkov, R. Lindau, E. Materna-Morris, A. Möslang, TEM characterization of precipitates in EUROFER 97, Prog. Nucl. Energy 57 (2012) 8–13.